CHALMERS

High Efficiency Heavy Duty Truck Engine

Master's Thesis in Solid and Fluid Mechanics

PAYAM BIGHAL

Department of Applied Mechanics
Division of Dynamics
CHALMERS UNIVERSITY OF TECHNOLOGY
Göteborg, Sweden 2012
Master's thesis 2012:39

MASTER'S THESIS IN SOLID AND FLUID MECHANICS

High Efficiency Heavy Duty Truck Engine

Payam Bighal

Department of Applied Mechanics
Division of Dynamics
CHALMERS UNIVERSITY OF TECHNOLOGY
Göteborg, Sweden 2012

High Efficiency Heavy Duty Truck Engine
PAYAM BIGHAL

Master's Thesis 2012:39
ISSN 1652-8557
Department of Applied Mechanics
Division of Dynamics
Chalmers University of Technology
SE-412 96 Göteborg
Sweden
Telephone: + 46 (0)31-772 1000

Department of Applied Mechanics
Göteborg, Sweden 2012

High Efficiency Heavy Duty Truck Engine
Master's Thesis in the Solid and Fluid Mechanics

PAYAM BIGHAL
Department of Applied Mechanics
Division of Dynamics
Chalmers University of Technology

ABSTRACT

The aim of this thesis work is to analyse the torsional vibration of a newly developed heavy duty truck engine to decrease the engine speed both at the idle speed and the cruising speed. New demands on fuel consumptions and CO_2 emissions force the manufacturers to develop engines operating at lower speeds. Down-speeding may result in several problems such as torsional vibration, increased engine speed fluctuation, difficulties to maintain boost pressure and high journal bearing loads. Dynamic characteristics of the mounting system have been optimized to avoid excessive deflection and bouncing of the engine. Stiffness and damping characteristics of mountings assumed to be linear and the system is considered to be one degree of freedom with harmonic excitation along the crankshaft axis. Moreover, the dynamic characteristics of flywheel and input shaft have been modified to prevent excessive torsional vibration and gear rattle in the powertrain system. Also conventional flywheel has been compared with dual-mass flywheel in down-speeding. The results showed that from torsional vibration point of view, downs-speeding was feasible. Furthermore dual-mass flywheels can significantly reduce the powertrain`s deflection up to 43%.

Key words: Down-speeding, Torsional vibration, Mounting system, Dual-mass flywheel

Contents

1 INTRODUCTION 5

2 METHODOLOGY 6

2.1 Engine Dynamics 6

2.2 Gas Force and Gas Torque 8
2.2.1 Single Cylinder 8
2.2.2 Multi-cylinder Engine 9

2.3 Inertia Force and Shaking Force 10
2.3.1 Single Cylinder 10
2.3.2 Multi-cylinder Engine 12

2.4 Inertia Torque, Shaking Torque and Moment 13
2.4.1 Single Cylinder 13
2.4.2 Multi-cylinder Engine 13

2.5 Total Engine Torque 14

2.6 Flywheel 14
2.6.1 Advantages of DMF over CF 14

2.7 Multi-cylinder Engine Designs 15

3 ANALYSIS OF POWERTRAIN MOUNTING SYSTEM 16

4 SOLVING STRATEGY 20

4.1 Bouncing 21

5 TORSIONAL VIBRATIONS ANALYSIS OF POWERTRAIN 23

5.1 Conventional Flywheel 25

5.2 Dual Mass Flywheel 29

6 COMPARISON 33

6.1 Conventional Flywheel 33
6.1.1 Inertia 1 33
6.1.2 Inertia 2 33
6.1.3 Torque 33

6.2 Dual-Mass Flywheel 33
6.2.1 Inertia 1 33
6.2.2 Inertia 2 33
6.2.3 Inertia 3 33
6.2.4 Torque 34

7 CONCLUSION AND FURTHER RESEARCH RECOMMENDATIONS 35

8 REFERENCES 36

Preface

This work is a part of a research project concerning down-speeding of heavy duty truck engine in cooperation with Volvo Powertrain. In this study, calculations have been done with MATLAB. The calculations have been carried out from September 2011 to November 2011. The project is carried out at the Department of Applied Mechanics, Dynamics, Chalmers University of Technology, Sweden.

The project has been carried out with Mr Eng. Thomas Klang, senior advisor of Volvo Powertrain as industry supervisor and Prof. Anders Bostrom as supervisor at Chalmers University. I would also like to thank Prof. Ingemar Denbratt, Hans Bondeson, Peter Nilsson and Hoda Yarmohammadi for their co-operation and involvement.

It should be noted that the thesis could never have been conducted without the professionalism of the Volvo staff.

Finally I wish to acknowledge the support of Mr Thomas Klang and Prof. Anders Bostrom. Also I would like to express my deepest gratitude to my mother for her unconditional support.

Göteborg February 2012

Payam Bighal

1 Introduction

High efficient internal combustion engines can be reached by applying different possible routes. Down-speeding is one of those routes that has been investigated and presented in this thesis work.

Down-speeding means operating the engine at lower speeds by means of changes through transmission and/or final drive ratio. It plays an important role in raising the efficiency since the engine friction and relative heat transfer will be reduced and also gas exchange losses will become smaller. Down-speeding is to achieve the same power needed to run the vehicle while the engine speed is being lowered. This can be achieved through two different ways:

First approach is to augment the boost power of the engine and second is through changing the dynamic configuration of the engine.

The latter procedure is more complicated and demands more changes in the configuration of the engine. Changes can be done to the slider-crank mechanism of the engine, i.e. piston and crank. Enlarging the piston area to have a bigger surface for combustible material to react, therefore obtain more pressure and consequently more force acting on the piston. Eventually more torque acting on the crankshaft, also extending crank to make the force at the crankpin have a bigger lever (moment arm) thus making bigger torque applied to the crankshaft. The first method is accomplished by rising up the engine torque by means of turbo chargers.

Conversely, down-speeding results in several problems such as torsional vibrations, problems with the powertrain mounting system, high journal bearing load, and increased engine speed fluctuation, difficulties to maintain boost pressure and NVH (Noise, Vibration and Harshness) problems.

For a given vehicle, a reduced engine speed means that the engine is operating at higher specific load; BMEP-Brake Mean Effective Pressure, which results in higher efficiency and thus reduced fuel consumption. The reasons for the increased efficiency are found in reduced engine friction, reduced relative heat transfer, less gas exchange losses and faster combustion (in crank angle degrees).

In this thesis work vibrations as a consequence of down-speeding have been investigated and verified to get the least noise and disturbances. Vibration abatement and controlling the oscillations have been studied and applied through modification of the engine mounting system characteristics and developing the transmission parts.

2 Methodology

2.1 Engine Dynamics

Internal combustion engines use two common combustion cycles; Clerk two-stroke cycle and Otto four-stroke cycle. The second, which is the most common in trucks and automobiles, takes four strokes of the piston to complete one cycle, that is, it takes 720^{o} of a crankshaft to complete one four-stroke cycle.

To study engine dynamics the kinematics of a typical slider-crank must first be considered, because each piston and its cylinder along with the connecting rod and the crank resemble a slider-crank mechanism except that the engine is "back-driven" compared to the common slider-crank linkage which is usually driven through the crank part by a rotary machine.

This slider-crank has motion aligned with the axis (X) which is perpendicular to the crankshaft and passes through the main pin thus called "non-offset" slider-crank. Assume the following parameters for the various parts according to figure 1.1:

$l : conrod\ length$
$r : crank\ radius$
$\theta : angle\ of\ the\ crank$
$\phi : angle\ between\ conrod\ and\ X - axis$
$x : instantaneous\ piston\ position$

For constant angular velocity of the crank, the angle can be given as $\theta = \omega t$. From geometry the following equations for position, velocity and acceleration of the piston can be deduced respectively:

$$x = r\cos\omega t + l\sqrt{1 - (\frac{r}{l}\sin\omega t)^2} \tag{2.1}$$

$$\dot{x} = -r\omega[\sin\omega t + \frac{r}{2l}\frac{\sin 2\omega t}{\sqrt{1 - \left(\frac{r}{l}\sin\omega t\right)^2}}] \tag{2.2}$$

$$\ddot{x} = -r\omega^2\{\cos\omega t - \frac{r[l^2(1 - 2\cos^2\omega t) - r^2\sin^4\omega t]}{[l^2 - (r\sin\omega t)^2]^{\frac{3}{2}}}\} \tag{2.3}$$

(Velocity and acceleration are obtained by differentiating position with respect to time and also assuming that ω is constant for steady-state analysis) [3, 4].

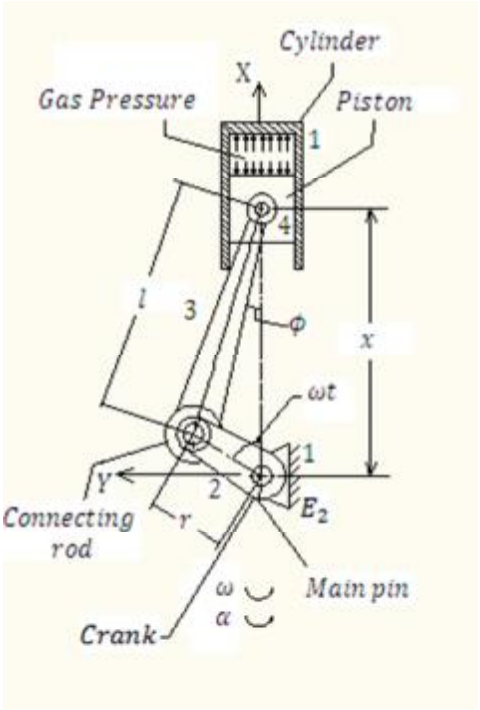

Figure 2.1 Four-bar slider-crank mechanism

Figure 1.1 shows a single cylinder as a fourbar slider-crank mechanism. Numbers in the figure depict each part in a way that 1 refers to the ground plane of a slider-crank mechanism which in an engine represents the cylinder and engine shell, 2 shows the crank, 3 illustrates the connecting rod and 4 represents the piston. Also the position of the main pin is shown by E_2.

To get more tangible effects of changes in parameters r and l it is better to derive simpler expressions, however, they become approximate. Using the binomial theorem to expand the radical in equation (2.1), equations for position, velocity and acceleration become respectively as follows:

$$x \cong l - \frac{r^2}{4l} + r\left(\cos\omega t + \frac{r}{4l}\cos 2\omega t\right) \tag{2.4}$$

$$\dot{x} \cong -r\omega\left(\sin\omega t + \frac{r}{2l}\sin 2\omega t\right) \tag{2.5}$$

$$\ddot{x} \cong -r\omega^2\left(\cos\omega t + \frac{r}{l}\cos 2\omega t\right) \tag{2.6}$$

Note that ω is assumed to be constant in deriving the velocity and acceleration formulas, therefore there is no angular acceleration (α) in the system. In this particular case the binomial expansion process leads to Fourier series expansion for the exact expressions of displacement, velocity and acceleration. Here we dropped the fourth, sixth and subsequent power terms of the binomial expansion because the error is less than one percent (for detailed information refer to [3, 4]).

There are several sources of dynamic excitation in the engine, namely forces and torques that ensue from explosive gas forces in the cylinder and inertia forces and torques which are due to the high speed motion of elements in the engine, specifically

pistons, cranks and conrods. Superposition of these forces and torques result in total force and torque of the engine. Here each of the components is analysed separately.

2.2 Gas Force and Gas Torque

2.2.1 Single Cylinder

The gas pressure which results from the exploding air-fuel mixture on top of the piston surface results in gas force. Considering piston area as A_p, P_g gas pressure and bore of cylinder as B, the gas pressure in the direction of the X-axis in figure 2.2 becomes:

$$F_g = -\frac{\pi}{4} P_g B^2 \tag{2.7}$$

The gas torque which is due to the gas force acting at a moment arm about the crank center (main pin) E_2 in figure 2.2 finally after some manipulations becomes:

$$T_g \cong F_g r \sin \omega t \left(1 + \frac{r}{l} \cos \omega t\right) \tag{2.8}$$

Note that the equation above is an approximation and is obtained by neglecting terms of crank/conrod ratio ($\frac{r}{l}$) higher than one. Consider that the friction is neglected also. For more detailed equations refer to [3].

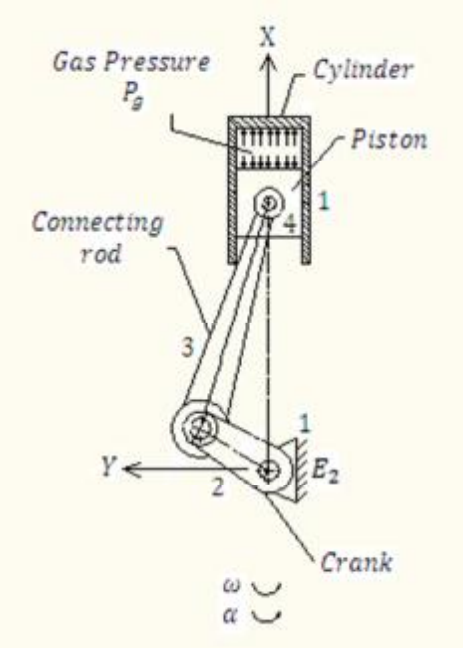

Figure 2.2 Four-bar slider-crank linkage as a schematic design of a single cylinder

2.2.2 Multi-cylinder Engine

By summing the contributions of n cylinders and every single phase-shifted by its power stroke angle we have the gas force for all cylinders as:

$$T_{g21}^{t} \cong F_g r \sum_{i=1}^{n} \left\{ \sin(\omega t - \Psi_i) \left[1 + \frac{r}{l} \cos(\omega t - \Psi_i) \right] \right\} \tag{2.9}$$

Where Ψ_i is the power stroke angle for cylinder i and n is the number of cylinders.

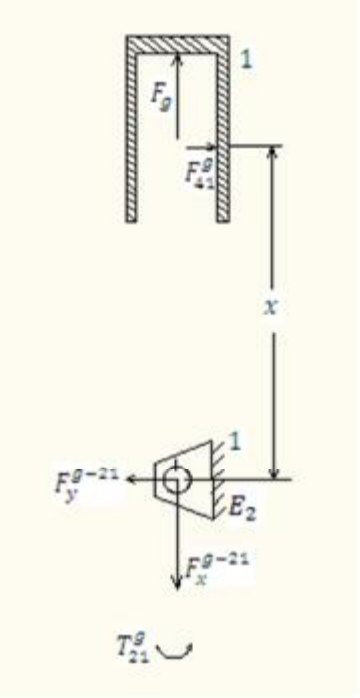

Figure 2.3 Gas force analysis of a single cylinder at ground plane

Figure 2.3 shows forces acting on the ground plane associated with the gas force. The force F_g is the gas force which acts on the cylinder and F_{41}^{g} is the force of the gas pressure acting on the surface of the piston perpendicular to the cylinder. Also the forces F_x^{g-21} and F_y^{g-21} are reaction forces on the main pin resulted from the gas pressure in the cylinder acting on the surface of the piston. (For more details refer to [3]).

2.3 Inertia Force and Shaking Force

2.3.1 Single Cylinder

In order to develop expressions for the inertia forces and torques which are due to the accelerations of elements in the engine, the slider-crank mechanism is simplified as a lumped mass model. The mentioned lumped mass model is as below:

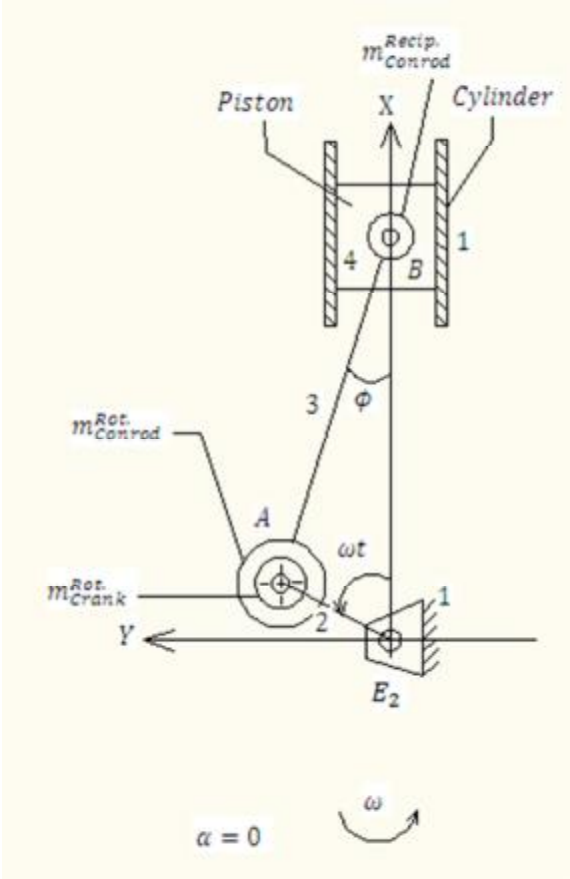

Figure 2.4 Lumped mass dynamic model of a single cylinder

$m^{Recip.}_{Conrod}$: *part of the conrod mass as a portion of the reciprocating mass*

$m^{Rot.}_{Conrod}$: *part of the conrod mass as a portion of the rotating mass*

$m^{Rot.}_{Crank}$: *crank mass as a portion of the rotating mass*

(In order to understand how these lumped masses are created refer to [3]). Presumptively $^1/_3$ of the mass of connecting rod plus the mass of piston, piston pin and piston rings constitute reciprocating mass (m_A) while $^2/_3$ of connecting rod plus crankpin form the rotational mass (m_B).

By using this lumped mass model the sum of inertia forces at points A and B construct the total inertia force as:

$$F_i = -m_A a_A - m_B a_B \tag{2.10}$$

Using equation (2.6) and considering that the acceleration of the piston is only in the X-direction this total force can be broken up into X and Y components (see figure 2.5):

$$F_{ix} \cong -m_A(-r\omega^2 \cos \omega t) \; - m_B[-r\omega^2(\cos \omega t + \frac{r}{l}\cos 2\omega t)] \tag{2.11}$$

$$F_{iy} \cong -m_A(-r\omega^2 \sin \omega t) \tag{2.12}$$

Note that the equations above are derived based on steady-state conditions so that there is no angular acceleration in the system, in other words the crank velocity ω is held constant.

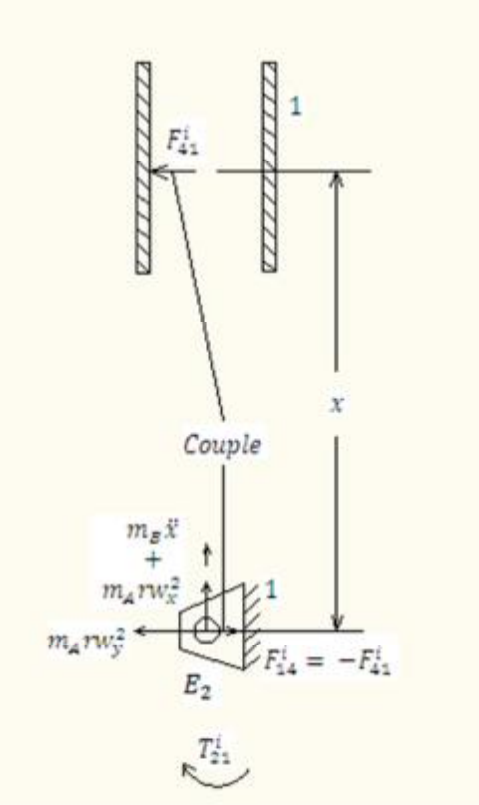

Figure 2.5 Analysis of inertia forces at ground plane for a single cylinder

Equations (2.11) and (2.12) are also defined as shaking forces with opposite sign (see figure 2.5) which are the sum of all forces acting on the ground plane which is here the engine compartment. It is noteworthy that the gas force does not contribute to shaking forces, because it will cancel within the mechanism according to figure 2.3; put differently only external and inertia forces contribute to shaking forces [3].

Consider that the inertia force F_{i41} which is the force of piston acting on the cylinder wall is cancelled within the mechanism; therefore it is not included in shaking forces. This inertia force always exists except at TDC (Top Dead Centre) and BDC (Bottom

Dead Centre) positions of the piston. Again friction has been ignored in the above considerations.

2.3.2 Multi-cylinder Engine

For an inline multi-cylinder engine with balanced crank the shaking force is:

$$F_s^t \cong m_B r\omega^2 \sum_{i=1}^{n} \left[\cos(\omega t - \phi_i) + \frac{r}{l}\cos 2(\omega t - \phi_i)\right] \qquad (2.13)$$

Where n is the number of cylinders and $\phi$is the phase angle which is zero for cylinder 1, i.e. $\phi_1 = 0$.

Recall that the expression above is approximate in that all harmonics above the second are dropped.

2.4 Inertia Torque, Shaking Torque and Moment

2.4.1 Single Cylinder

2.4.1.1 Inertia and Shaking Torque

Inertia forces acting at a moment arm contribute to the inertia torque. Again ignoring friction and assuming that ω is constant, mass A in figure 2.4 will not result in an inertia torque; because of the two components which act at point$A$, one is radial which has no moment arm and the other which is tangential includes angular acceleration that is zero in this case. On the contrary, the inertia force at point B creates a couple with a force equal but with opposite sign at point E_2, which their moment arm is the instantaneous position of the piston (x) , according to figure 2.5 this inertia torque is:

$$T_{i21} = F_{i41}.x \tag{2.14}$$

Finally after some manipulations it becomes:

$$T_{i21} \cong \frac{1}{2} m_B r^2 \omega^2 \left(\frac{r}{2l}\sin\omega t - \sin 2\omega t - \frac{3r}{2l}\sin 3\omega t\right) \tag{2.15}$$

The inertia torque is equal to the shaking torque and its average value is always zero. Thus it does not affect the driving torque and the only thing it does is increasing the vibration in the system as it creates positive and negative oscillations in the total torque. The effects of the inertia torque or the shaking torque can be reduced or eliminated by proper arrangement of the cylinders in a multi-cylinder engine.

2.4.2 Multi-cylinder Engine

2.4.2.1 Inertia Torque

For an inline multi-cylinder engine with balanced crank the inertia torque is:

$$T_{i21}^{t} \cong \frac{1}{2} m_B r^2 \omega^2 \sum_{i=1}^{n} \left[\frac{r}{2l}\sin(\omega t - \emptyset_i) - \sin 2(\omega t - \emptyset_i) - \frac{3r}{2l}\sin 3(\omega t - \emptyset_i)\right] \tag{2.16}$$

As is mentioned before this detrimental torque is not affecting the net driving torque and can be reduced or almost eliminated by proper choice of phase angle and with a sufficient flywheel; nevertheless it exists within the crankshaft and if the crankshaft is not designed properly it can lead to fatigue failure. [3]

2.4.2.2 Shaking Moment

Contrary to the single cylinder which is located in a single plane and is statically balanced, in multi-cylinder engines due to three dimension system and having several cylinders in different planes along the crankshaft and perpendicular to it, we cannot have static balance. Although we may have shaking forces cancelled, there is unbalanced moments in the engine block`s plane. These harmful moments together can be cancelled to some extend by proper phase angle; however, changing phase angle may influence the effect of shaking torques and shaking forces. Therefore a good trend must be implemented to have the least effect of them; in other words there should be compensation to have the best design. Reader may refer to [3, 4] for further information.

2.5 Total Engine Torque

The sum of the inertia torque and the gas torque constitutes the total engine torque. Consider that the contribution of each of these depends on the speed of the engine, so that the gas torque comparing to inertia torque is less sensitive to speed and is dominant at low speed. Therefore at low engine speeds, the inertia torque, which is the dominating portion of the total engine torque at high speeds, can be neglected.

2.6 Flywheel

Flywheels are parts which can store rotational energy. They display big inertia that is resistance against any change in its state of motion. These rotational mechanical devices are used mainly in reciprocating engines. Because the energy source is not continuous in time, therefore utilizing these mechanical devices can significantly reduce large oscillations in the torque-time function thereby provide continuous energy. [3, 13]

Nowadays two types of flywheels are used in the industry:

- Conventional Flywheel
- Dual Mass Flywheel

A conventional flywheel (CF) usually consists of a single flat disk and a Dual-Mass Flywheel (DMF) consists of two sections, primary mass and secondary mass. These masses are connected to each other in a way so that they can move with respect to other to a certain degree. Each type is bolted at one side to the crankshaft; in DMF the primary mass, and the other side is bolted to the clutch; in DMF the secondary mass.

2.6.1 Advantages of DMF over CF

1. Having two different masses; two different sections, isolates vibration in the crankshaft from passing on to the second mass to some extent. Thereby preventing undesirable vibrations in the gear box, thereupon preventing gear rattle
2. Immediate react to increased load amplitude
3. Due to the existence of a medium in DMF, between primary and secondary mass; and configuration of throttle geometry DMF can be adapted to different requirements better than CFs

Important effects of DMFs can be stated as:

1. Reduce booming noise and gear rattle by introducing torsion damper
2. Lower fuel consumption by allowing lower engine idle speed
3. Avoid engine and transmission vibration system`s resonance speed by shifting it to below the idle speed
4. Protect transmission components by reducing engine irregularity and reduction of primary mass compared to one integrated flywheel

Note that such a DMF with maximum effect is highly non-linear. [7, 8, 9]

2.7 Multi-cylinder Engine Designs

There are several configurations for multi-cylinder engines, namely “INLINE Engines”, “VEE Engines”, “ROTARY Engines”, “OPPOSED Engines” and “RADIAL Engines”. From all these arrangements “INLINE Engines” is the most common and simplest; the engine under consideration in this thesis is also of this type. In this arrangement as can be deduced from its name all cylinders are in a common plane. This arrangement gives the simplest way to alleviate unbalancing and shaking forces in the engine. [9]

3 Analysis of powertrain mounting system

In the current approach on behalf of simplicity, the mounting system is considered as a one degree of freedom rotational system, consisting of one torsional spring and an inertia representing the mounting and the engine, respectively. However, the original system is comprised of five mounts with three in front and two at the rear of the engine, the mentioned approach can satisfy our goal with nearly the same precision as the original system.

The objective which is laid out in this approach is to find appropriate stiffness for mounts that can assure the following requirements:

- Avoid resonance at low speeds
- Stand engine weight
- Avoid engine bouncing

It is noteworthy that noise and vibration, which are adverse phenomena in the engine system, enforce mounts to have conflicting characteristics for their best isolation performance [1]. So that to isolate noise and forces transmitted by the engine to the vehicle structure, lower stiffness and damping is desired; on the contrary at lower speeds, typically idle speed, to isolate road induced vibrations, higher stiffness and damping is required. Care should be taken that reducing the mounting stiffness below a certain value will lead to rigid body motion in the model. This means that the mounts cannot fulfil their very first task that is to carry the engine load and restrict the relative motion of it, particularly bouncing [6].

In this thesis due to considering down-speeding effects on engine compartment, only vibration is taken into account which is the dominant consequence of this approach. The system under consideration consists of only one mount and the engine, which is assumed that behaviour of the mount dynamic characteristics, stiffness and damping, are linear; also presumed that the mount is massless.

As was mentioned the system under consideration is a 1 DOF system; therefore the governing equation for motion is as follows:

$$I\ddot{\varphi} + C\dot{\varphi} + K\varphi = T(t) \tag{3.1}$$

Where:

I : $moment\ of\ inertia(kgm^2)$

C : $Damping\ Coefficient(Nms/Rad)$

K : $Stiffness(Nm/Rad)$

T : $External\ Torque\ on\ the\ System(Nm)$

φ : $Deflection\ of\ the\ System(Rad)$

In this case "I" is the inertia of the engine which is $103\ \mathrm{kgm}^2$ and the external torque is the engine torque which is sum of a static torque and a harmonic one:

$$T(t) = T_0 + T_0\sin(3\omega t) \tag{3.2}$$

Notice that however the engine angular speed is ω but in equation (3.2) "3ω" is used which is called 3rd order of sinusoidal term, this is because of the number of cylinders that have power stroke at each revolute of the crankshaft i.e. frequency of the excitation depends on half of the number of cylinders of the engine. By this definition an engine with 4 cylinders has an excitation frequency of 2nd order and an 8 cylinder engine has an excitation of 4th order.

Solution of (3.1) comprises two parts: Complementary function which is the solution of homogenous equation and particular integral.

$$\varphi = \varphi_{hom} + \varphi_{Part} \tag{3.3}$$

In this case complementary function is free damped vibration:

$$I\ddot{\varphi} + C\dot{\varphi} + K\varphi = 0 \tag{3}$$

General solution to equation (3) is given by:

$$\varphi_{hom} = e^{-\left(\frac{C}{2I}\right)t}\left[Ae^{t\sqrt{\left(\frac{C}{2I}\right)^2-\frac{K}{I}}} + Be^{-t\sqrt{\left(\frac{C}{2I}\right)^2-\frac{K}{I}}}\right] \tag{3.4}$$

"A" and "B" are constants which are defined by initial conditions.

Statements under the radical can be positive, zero or negative. Based on mentioned cases three dynamic situations will happen: over-damped, critical damped or under-damped, respectively.

In this approach the under-damped case is studied which is the case where $\xi < 1$ then the equation (3.4) can be written in the form:

$$\varphi_{hom} = e^{-\xi\omega_n t}\left[Ae^{i\omega_n t\sqrt{(1-\xi^2}} + Be^{-i\omega_n t\sqrt{(1-\xi^2}}\right] \tag{3.5}$$

Since

$$\frac{C}{I} = 2\xi\omega_n \tag{3.6}$$

$$\frac{K}{I} = \omega_n^2 \tag{3.7}$$

This finally after some manipulations leads to the following equation including initial conditions:

$$\varphi_{hom} = e^{-\xi\omega_n t}\left[\frac{\dot{\varphi}(0) + \xi\omega_n\varphi(0)}{\omega_n\sqrt{1-\xi^2}} + \sin\left(\omega_n t\sqrt{1-\xi^2}\right) + \varphi(0)\cos\left(\omega_n t\sqrt{1-\xi^2}\right)\right] \tag{3.8}$$

This equation shows that the damped oscillation frequency is:

$$\omega_d = \frac{2\pi}{\tau_d} = \omega_n\sqrt{1-\xi^2} \tag{3.9}$$

(The reader may refer to [1, 2] for detailed information).

The particular solution of equation (3.1) with harmonic excitation, T, is a steady-state oscillation with frequency ω equal to the excitation frequency. It can be assumed that the solution is:

$$\varphi_{Part} = \phi \sin(\omega t - \beta) \tag{3.10}$$

ϕ is the amplitude of oscillation and β is the phase angle with respect to the excitation torque.

Amplitude and phase angle in the previous equation can be derived by inserting equation (3.10) into (9):

$$\phi = \frac{T_0}{\sqrt{(K - I\omega^2)^2 + (C\omega)^2}} \tag{3.11}$$

and

$$\beta = \tan^{-1} \frac{C\omega}{K - Iw\omega^2} \tag{3.12}$$

Using equations (3.6) and (3.7) the amplitude and phase angle may be written in the form below:

$$\frac{\phi K}{T_0} = \frac{1}{\sqrt{\left[1 - \left(\frac{\omega}{\omega_n}\right)^2\right]^2 + \left[2\xi\left(\frac{\omega}{\omega_n}\right)\right]^2}} \tag{3.13}$$

and

$$\tan\phi = \frac{2\xi\left(\frac{\omega}{\omega_n}\right)}{1 - \left(\frac{\omega}{\omega_n}\right)^2} \tag{3.14}$$

Equations (3.13) and (3.14) are called the non-dimensional amplitude and phase angle, respectively.

Finally by inserting (3.11) in form of (3.13) into (3.10) the particular solution of (3.1) can be written:

$$\varphi_{Part} = \frac{T_0}{K} \frac{\sin(\omega t - \beta)}{\sqrt{\left[1 - \left(\frac{\omega}{\omega_n}\right)^2\right]^2 + \left[2\xi\left(\frac{\omega}{\omega_n}\right)\right]^2}} \tag{3.15}$$

Thus the total solution becomes:

$$\varphi = \frac{T_0}{K}\frac{\sin(\omega t-\beta)}{\sqrt{\left[1-\left(\frac{\omega}{\omega_n}\right)^2\right]^2+\left[2\xi\left(\frac{\omega}{\omega_n}\right)\right]^2}} + e^{-\xi\omega_n t}\left[\frac{\dot{\varphi}(0)+\xi\omega_n\varphi(0)}{\omega_n\sqrt{1-\xi^2}}+\sin\left(\omega_n t\sqrt{1-\xi^2}\right) + \varphi(0)\cos\left(\omega_n t\sqrt{1-\xi^2}\right)\right] \quad (3.16)$$

According to vibration analysis principles when the natural frequency of the system is equivalent to the excitation frequency we will have resonance in our system [1, 2] which is undesirable. Therefore avoiding this destructive phenomenon is our priority in this section of the thesis work.

Based on criteria when the natural frequency is lower than the excitation frequency divided by the square root of two, that zone is safe and far from the resonance as follows [1, 2]:

$$\frac{3\omega}{\omega_n} > \sqrt{2} \quad (3.17)$$

$$\omega_n = \sqrt{\frac{K}{I}} \quad (3.18)$$

In other words equations (3.17) and (3.18) guarantee that the non-dimensional amplitude (3.13) is smaller than 1.

Here natural frequency is the undamped natural frequency which makes the analysis conservative according to following relation between damped and undamped natural frequency:

$$\omega_d = \omega_n\sqrt{1-\xi^2} \quad \rightarrow \quad \omega_d < \omega_n \quad \rightarrow \quad \frac{3\omega}{\omega_d} > \sqrt{2} \quad (3.19)$$

The above criteria together with the limitation for damping factor which is 10% of critical damping are constructing our strategy to gain mounting system applicable for down-speeding.

4 Solving Strategy

Equation (3.1) can be written in the following form:

$$\ddot{\varphi} + 2\xi\omega_n\dot{\varphi} + \omega_n^2\varphi = T(t)/I \tag{4.1}$$

This form of the momentum equation shows its dependency on the natural frequency.

A starting value for the stiffness is obtained at 600 rpm engine speed which is equivalent to 10 Hz engine frequency and consequently 30 Hz of excitation frequency. At this speed the stiffness is "1.830×10^6 Nm/rad".

Thus the analysis is performed by lowering the stiffness from its starting value and verifying whether the corresponding natural frequency is bounded within our safe zone or not. Each safe zone is defined regarding the designated engine speed to the system, in other words at each speed the frequency of excitation torque will change, accordingly care should be taken to always have equation (3.17) true.

Five different engine speeds is considered according to the following table:

Table 4.1 Engine speed range under consideration for analysis of the mounting system

Engine speed (Rpm)	480	540	600	800	1000
Engine Frequency (Hz)	8	9	10	13.333	16.666
Safe zone's lower bound (Hz)	16.97	19.09	21.21	28.28	35.35

Again notice that the engine frequency is different from the excitation frequency which is three times the engine frequency.

4.1 Bouncing

Another criterion in decreasing mounting stiffness is bouncing which particular care must be taken to avoid. If the stiffness of the mounts becomes too low, the engine could hit the cabin or may even bounce, hence static displacement must be measured to guarantee dynamic characteristic of the mounts. Static displacement is the ratio of static torque to stiffness.

$$U_0 = {}^{T_0}/_{K} \tag{4.2}$$

Table 4.2 ensures that the designated stiffness is in-bound and acceptable.

Table 4.2 Static displacement, stiffness and natural frequency of the mounting system

Natural Frequency f_n (Hz)	Stiffness K (Nm/rad)	Static Displacement (Degree)
21.213	1.830×10^{6}	3.860×10^{-2}
20.676	1.740×10^{6}	3.955×10^{-2}
20.125	1.647×10^{6}	4.175×10^{-2}
19.558	1.555×10^{6}	4.420×10^{-2}
18.974	1.464×10^{6}	4.697×10^{-2}
18.371	1.372×10^{6}	5.010×10^{-2}
17.748	1.281×10^{6}	5.368×10^{-2}
17.103	1.190×10^{6}	5.781×10^{-2}
16.432	1.098×10^{6}	6.262×10^{-2}
15.732	1.006×10^{6}	6.832×10^{-2}
15.000	9.150×10^{5}	7.515×10^{-2}
14.230	8.234×10^{5}	8.350×10^{-2}

Considering the mentioned criteria, the engine span and based on the table 4.1 results was obtained for engine deflection at each speed and related stiffness and natural frequency of the system which is tabulated below:

Table 4.3 Deflection of the mounting system at different engine speed and stiffness

Radial Frequency ω_n (rad/s)	Natural Frequency f_n (Hz)	Stiffness K (Nm/rad)	Engine Speed Spam under Consideration (Hz)				
			8	9	10	13.333	16.666
			Deflection (Degree)				
1.333×10^2	21.213	1.830×10^6	x	x	x	0.0138	0.0082
1.299×10^2	20.676	1.740×10^6	x	x	0.0346	0.0136	0.0081
1.264×10^2	20.125	1.647×10^6	x	x	0.0331	0.0133	0.008
1.229×10^2	19.558	1.555×10^6	x	x	0.0317	0.0131	0.008
1.192×10^2	18.974	1.464×10^6	x	0.0442	0.0305	0.0129	0.0079
1.154×10^2	18.371	1.372×10^6	x	0.0419	0.0293	0.0127	0.0078
1.115×10^2	17.748	1.281×10^6	x	0.0398	0.0282	0.0124	0.0077
1.075×10^2	17.103	1.190×10^6	x	0.0379	0.0272	0.0122	0.0076
1.032×10^2	16.432	1.098×10^6	0.0534	0.0362	0.0262	0.012	0.0076
9.885×10^1	15.732	1.006×10^6	0.0501	0.0346	0.0254	0.0119	0.0075
9.425×10^1	15.000	9.150×10^5	0.0471	0.0331	0.0246	0.0117	0.0074
8.941×10^2	14.230	8.234×10^5	0.0444	0.0318	0.0239	0.0115	0.0073

The boxes marked by “x” in table (4.3) indicate that the designated stiffness for the mounting system at those speeds is unacceptable and out-of-bound.

5 Torsional vibrations analysis of powertrain

The purpose of analysing torsional vibrations of the powertrain is to get the least noise transferred to the cabin, protect transmission components by reducing engine irregularity and prevent gear rattle in the gear box.

Analysis of the powertrain is performed for two configurations:

1. Conventional Flywheel (CF)
2. Dual Mass Flywheel (DMF)

For the sake of simplicity the modelling system is considered as 2-DOF and 3-DOF, respectively. However the complete powertrain model is more complicated than the considered types; due to insignificant difference, it is acceptable to use the mentioned models. The complete model can be shown as below:

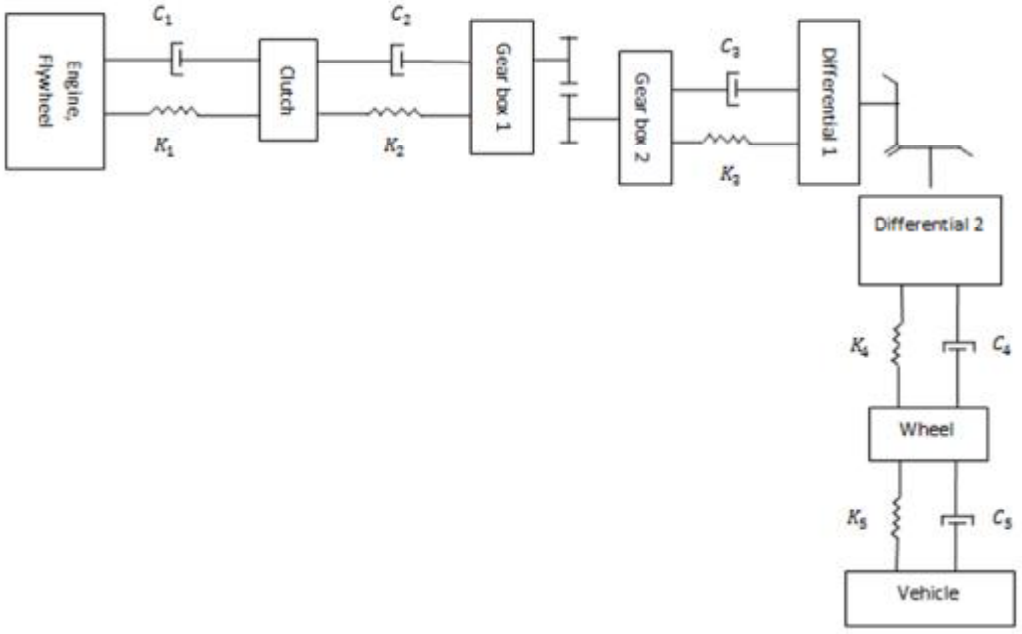

Figure 5.1 Schematic design of full powertrain torsional model

Notice that due to gear ratios in the gear box and differential it is difficult to solve the system of equations in this model. Therefore to solve such a model one should transform inertia and dynamic characteristics to the prior side of the gear sets. The schematic model which is shown below helps to accomplish this target:

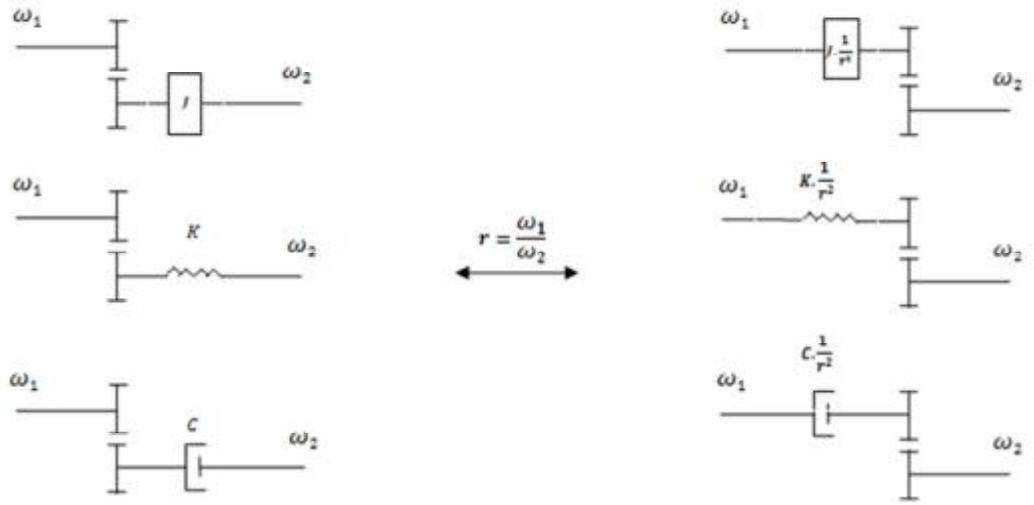

Figure 5.2 Transferring methods for inertia, springs and dampers

According to above the inertia model, springs and dampers after the gear set 1 and 2 transformed based on the gear ratio"r". It means that in order to have them at the left side of the gear set, they should be multiplied by the squared inverse of gear ratio. Eventually the simplified model without gear ratios is obtained:

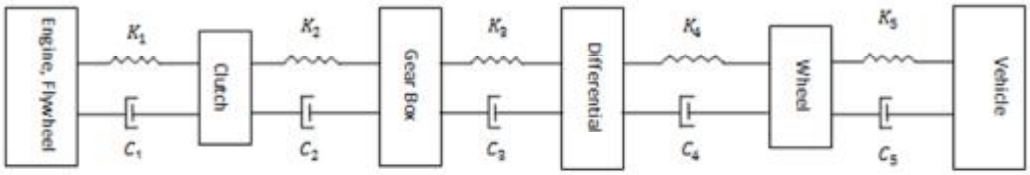

Figure 5.3 Schematic design of full powertrain model with integrating gear sets

It is obvious that with the gear ratio higher than one, inertia, spring and dampers become smaller compared to the previous quantity and with a gear ratio lower than 1, they become greater than the original quantity.

In all the following approaches, analyses are done based on the assumption that the crankshaft is sufficiently rigid so that all the torque is transformed to its subsequent component; thus no loss occurs.

5.1 Conventional Flywheel

In this approach the engine, flywheel and clutch are considered as a single inertia (rotational mass) and also the gear box and its housing. The scheme of this approach is as below:

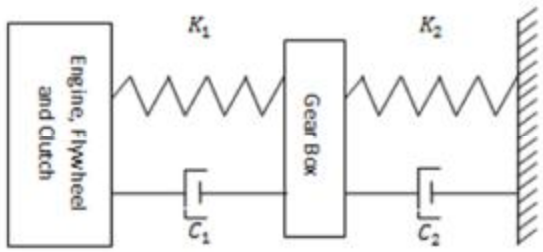

Figure 5.4 Schematic design of 2DOF powertrain torsional model

In figure 4.4 $K_1$and C_1 are the stiffness and damping characteristics of the clutch and K_2 and C_2 are the stiffness and damping characteristics of the driveshaft (prop-shaft).

In such a system we have two eigenvalues and therefore two natural frequencies. Here in contrary to the mounting system avoiding resonance is only the objective at the first vibration mode of the system, so that with adequate damping we can diminish negative effects of the resonance at the second mode. The reason to avoid only the fundamental mode can be described by the amplitude of the deflection and infeasibility; i.e. at higher modes which can be stated as higher frequencies the amplitude of the deflection is lower, therefore neutralizing resonance becomes possible by means of appropriate damping. Also the latter indicates that avoiding the second resonance is almost impossible since the dynamic characteristics of inertia are coupled. That is, changing stiffness properties of inertia will affect each natural frequency so the system is restricted to have one natural frequency out of excitation domain at the same time. Thus according to the above statements preventing first resonance is prior to the second one.

In this section the inertia of the system (inertia 1 as overall inertia of the engine, flywheel and clutch and inertia 2 as inertia of the gear box) with three configurations for dynamic characteristics in a wider range of engine speed has been considered. The damping ratios (ξ) for this system are 15.7 and 3.03 percent of critical damping. At each table damping and stiffness characteristics of the clutch and prop-shaft and natural frequency of the system are shown. Data for all configurations are tabulated in tables 5.1, 5.2 and 5.3:

Table 5.1 First configuration of the torsional system with CF

Object Number	1	2
Inertia (kgm^2)	3.97	1.06
Damping (Nms/rad)	0	36.8
Stiffness (Nm/rad)	1.70×10^4	8.20×10^4
Natural Frequency (Hz)	9.440	48.838

Table 5.2 Second configuration of the torsional system with CF

Object Number	1	2
Inertia (kgm^2)	3.97	1.06
Damping (Nms/rad)	0	36.8
Stiffness (Nm/rad)	1.70×10^4	9.00×10^4
Natural Frequency (Hz)	9.519	50.742

In this configuration inertia and damping is the same as configuration 1, only prop-shaft stiffness has changed and is increased to 9.00×10^4 Nm/rad.

Table 5.3 Third configuration of the torsional system with CF

Object Number	1	2
Inertia (kgm^2)	3.8	0.4
Damping (Nms/rad)	0	36.8
Stiffness (Nm/rad)	1.65×10^4	1.50×10^4
Natural Frequency (Hz)	7.132	45.320

With the data available steady state amplitudes has been obtained with the help of MATLAB. Notice that the dimension is in degrees.

The results for inertia i.e. the engine, flywheel and clutch as inertia 1 and the gear box as inertia 2 have been plotted at different configurations for comparison at figures 5.5 and 5.6.

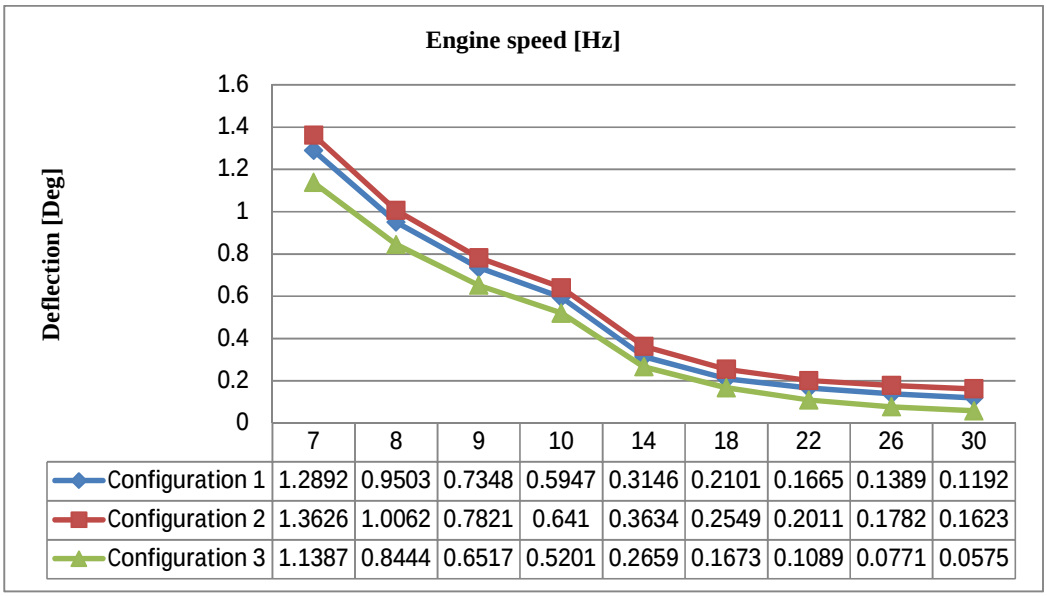

	7	8	9	10	14	18	22	26	30
Configuration 1	1.2892	0.9503	0.7348	0.5947	0.3146	0.2101	0.1665	0.1389	0.1192
Configuration 2	1.3626	1.0062	0.7821	0.641	0.3634	0.2549	0.2011	0.1782	0.1623
Configuration 3	1.1387	0.8444	0.6517	0.5201	0.2659	0.1673	0.1089	0.0771	0.0575

Figure 5.5 Steady state amplitude of deflection at inertia 1

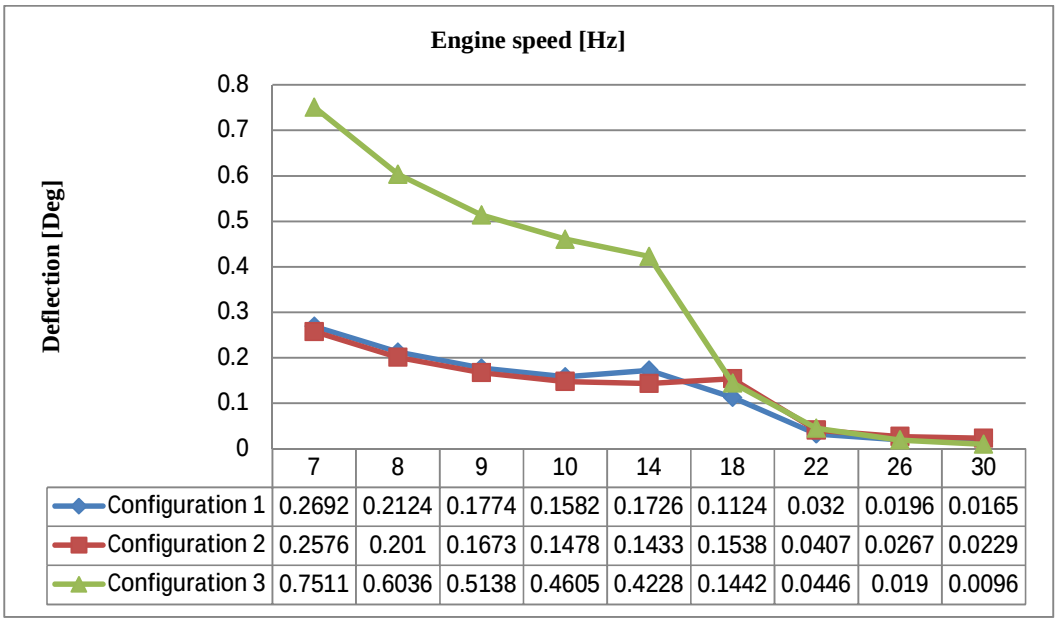

	7	8	9	10	14	18	22	26	30
Configuration 1	0.2692	0.2124	0.1774	0.1582	0.1726	0.1124	0.032	0.0196	0.0165
Configuration 2	0.2576	0.201	0.1673	0.1478	0.1433	0.1538	0.0407	0.0267	0.0229
Configuration 3	0.7511	0.6036	0.5138	0.4605	0.4228	0.1442	0.0446	0.019	0.0096

Figure 5.6 Steady state amplitude of deflection at inertia 2

The horizontal axis in the figures shows the engine speed at different levels in (Hertz) and vertical axis is the amplitude of the deflection in (degrees) at steady state. The table under each figure depicts the steady state deflection amplitude of the engine at each engine speed.

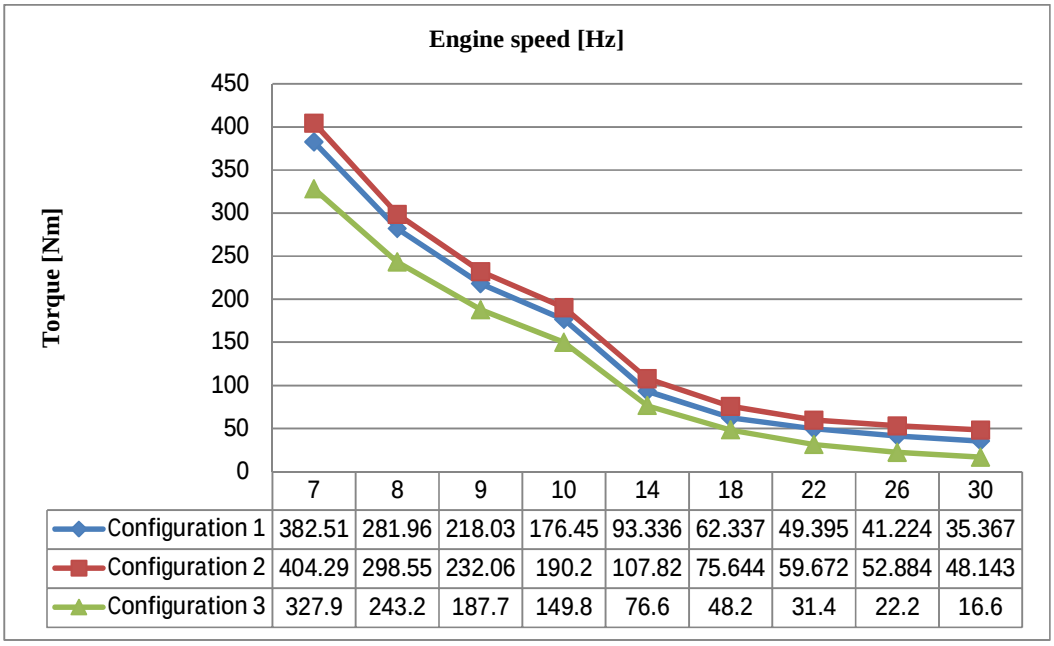

	7	8	9	10	14	18	22	26	30
Configuration 1	382.51	281.96	218.03	176.45	93.336	62.337	49.395	41.224	35.367
Configuration 2	404.29	298.55	232.06	190.2	107.82	75.644	59.672	52.884	48.143
Configuration 3	327.9	243.2	187.7	149.8	76.6	48.2	31.4	22.2	16.6

Figure 5.7 Steady state amplitude of input shaft`s torque

Figure 5.7 depicts steady state torque amplitude of the input shaft versus the engine speed. Also the table beneath this figure shows torque amplitude values at different configurations.

5.2 Dual Mass Flywheel

This approach is considered as a 3-DOF model in which the engine and primary flywheel construct the first inertia, the secondary flywheel and the clutch create the other inertia and the gear box and its housing is considered as the last inertia. The scheme of this approach is as below:

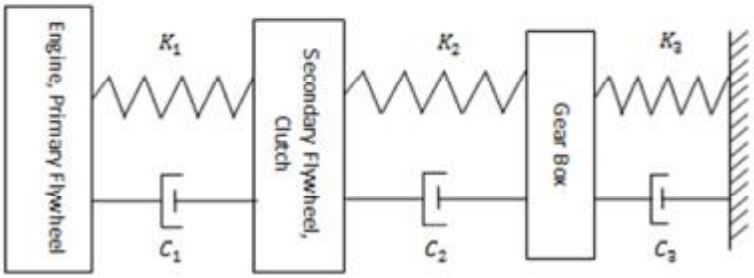

Figure 5.8 Schematic design of 3DOF powertrain torsional model

In such a system we have three eigenvalues. Similar to the system with conventional flywheel, in this system only the first resonance is prevented and the other two must be damped, but unlike the previous system it is feasible to shift the second and third resonance outside the engine`s excitation frequency span, although the production costs may not be justified.

In this section, as in section 5.1, the three configurations for dynamic characteristics in a wider range of the engine speed have been considered for all inertia. The damping factors for this system are 6.79, 12.95 and 3.16 percent of critical damping. Data for all configurations have been tabulated in tables 5.4, 5.5 and 5.6:

Table 5.4 First configuration of the torsional system with DMF

Object Number	1	2	3
Inertia (kgm^2)	1.8	0.6	0.5
Damping (Nms/rad)	30	0	36.8
Stiffness (Nm/rad)	2.00×10^4	1.10×10^4	3.50×10^4
Natural Frequency (Hz)	8.370	35.970	50.564

Table 5.5 Second configuration of the torsional system with DMF

Object Number	1	2	3
Inertia (kgm^2)	1.8	0.6	1.1
Damping (Nms/rad)	30	0	36.8
Stiffness (Nm/rad)	1.50×10^4	1.90×10^4	7.50×10^4
Natural Frequency (Hz)	9.835	34.705	50.099

Table 5.6 Third configuration of the torsional system with DMF

Object Number	1	2	3
Inertia (kgm^2)	2.2	0.5	0.9
Damping (Nms/rad)	30	0	36.8
Stiffness (Nm/rad)	1.50×10^4	2.50×10^4	7.00×10^4
Natural Frequency (Hz)	9.499	37.690	57.984

With the same procedure that has been taken for the conventional flywheel, section 5.1; results were obtained for Dual Mass Flywheel.

The results for all inertia i.e. engine and primary flywheel as inertia 1, secondary flywheel and clutch as inertia 2 and gear box as inertia 3 have been plotted at different configurations for comparison in figures 5.9 to 5.11. Again the horizontal axis shows the engine speed at different levels in Hertz and the vertical axis is the amplitude of deflection at steady state in degrees. The table under each figure depicts the steady state deflection amplitude of the engine at each engine speed.

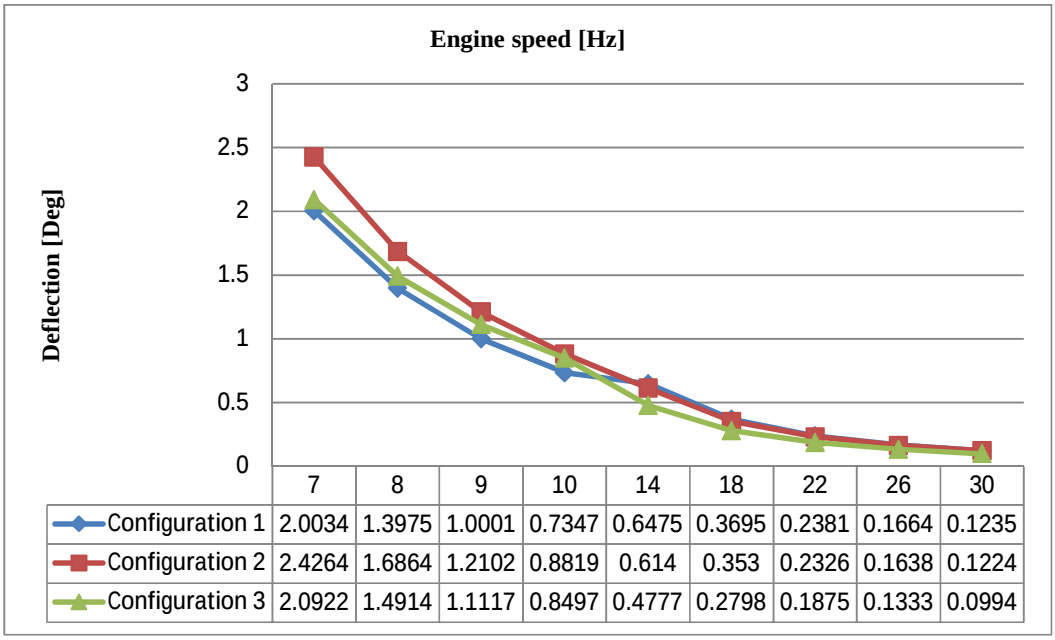

	7	8	9	10	14	18	22	26	30
Configuration 1	2.0034	1.3975	1.0001	0.7347	0.6475	0.3695	0.2381	0.1664	0.1235
Configuration 2	2.4264	1.6864	1.2102	0.8819	0.614	0.353	0.2326	0.1638	0.1224
Configuration 3	2.0922	1.4914	1.1117	0.8497	0.4777	0.2798	0.1875	0.1333	0.0994

Figure 5.9 Steady state amplitude of deflection at inertia 1

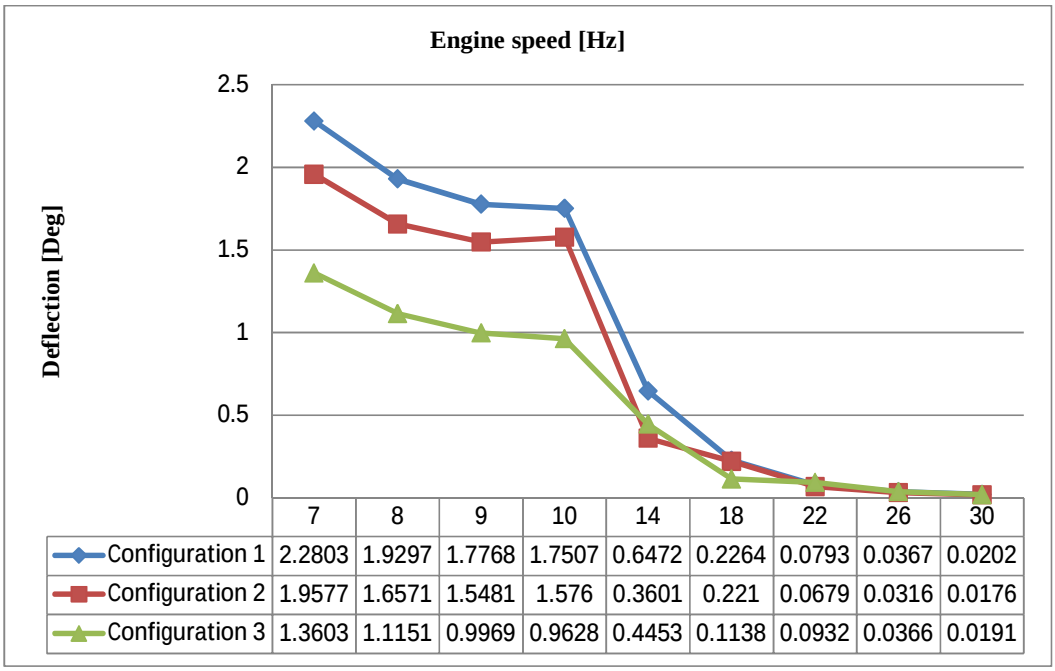

	7	8	9	10	14	18	22	26	30
Configuration 1	2.2803	1.9297	1.7768	1.7507	0.6472	0.2264	0.0793	0.0367	0.0202
Configuration 2	1.9577	1.6571	1.5481	1.576	0.3601	0.221	0.0679	0.0316	0.0176
Configuration 3	1.3603	1.1151	0.9969	0.9628	0.4453	0.1138	0.0932	0.0366	0.0191

Figure 5.10 Steady state amplitude of deflection at inertia 2

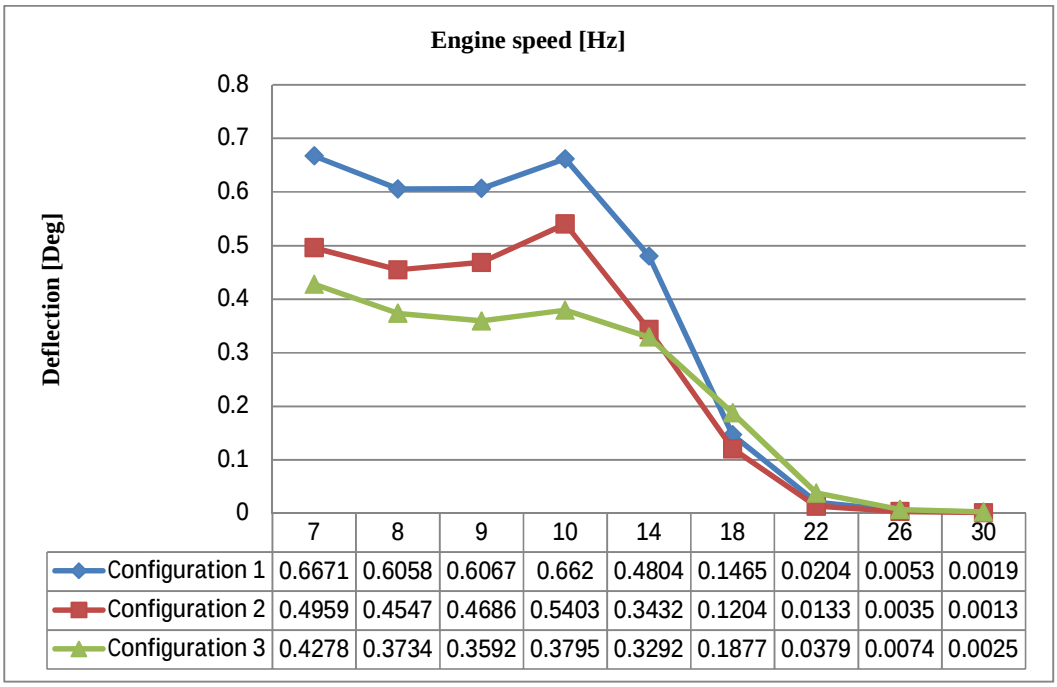

	7	8	9	10	14	18	22	26	30
Configuration 1	0.6671	0.6058	0.6067	0.662	0.4804	0.1465	0.0204	0.0053	0.0019
Configuration 2	0.4959	0.4547	0.4686	0.5403	0.3432	0.1204	0.0133	0.0035	0.0013
Configuration 3	0.4278	0.3734	0.3592	0.3795	0.3292	0.1877	0.0379	0.0074	0.0025

Figure 5.11 Steady state amplitude of deflection at inertia 3

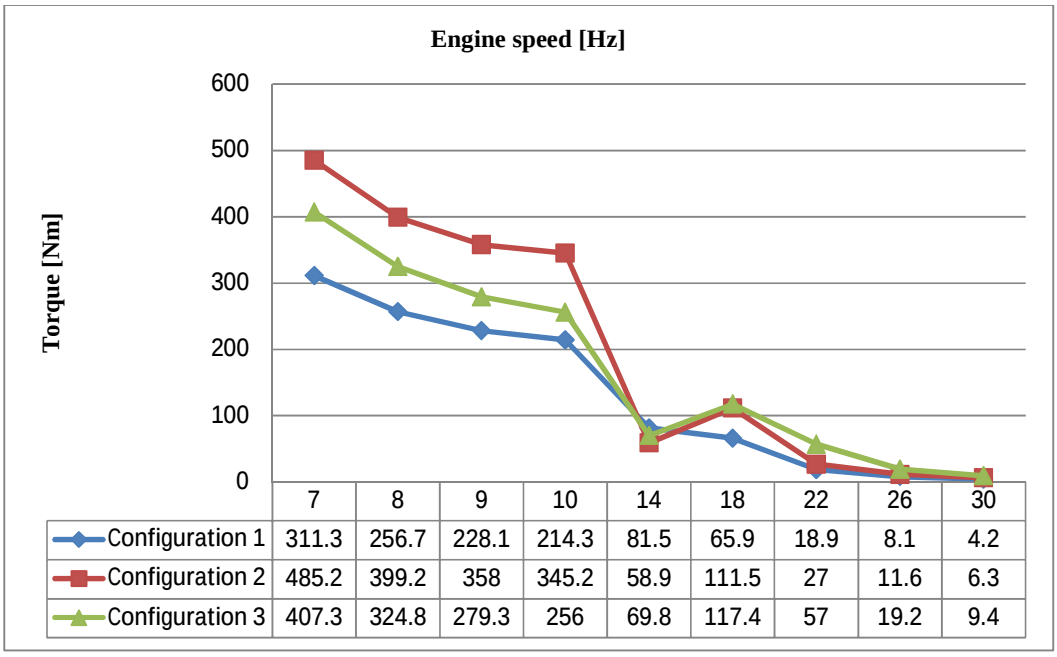

	7	8	9	10	14	18	22	26	30
Configuration 1	311.3	256.7	228.1	214.3	81.5	65.9	18.9	8.1	4.2
Configuration 2	485.2	399.2	358	345.2	58.9	111.5	27	11.6	6.3
Configuration 3	407.3	324.8	279.3	256	69.8	117.4	57	19.2	9.4

Figure 5.12 Steady state amplitude of input shaft`s torque

The steady state torque amplitude of the input shaft at the engine speed under consideration has been plotted in figure 5.12.

Similar to figure (5.7) in section 5.1, the vertical axis in figure 5.12 represents the torque amplitude in Nm and the vertical axis demonstrates the engine speed frequency from 7 Hz to 30 Hz equivalent to 420 rpm and 2100 rpm of the crankshaft speed, respectively. Also table beneath this figure shows torque amplitude values at different configurations for each speed.

6 Comparison

6.1 Conventional Flywheel

6.1.1 Inertia 1

Figure 4.5 demonstrates that configuration 3 has the lowest deflection among all configurations. It also shows that configuration 2 has the highest deflection. By studying the results one could deduce that the deflection at each configuration follow the same pattern and decrease with increasing engine speed (frequency). This is because the system stiffness and damping has been held constant during different engine frequencies.

6.1.2 Inertia 2

The deflection for the second inertia shows a completely different manner in comparison to the first inertia. Here configuration 3 has the highest deflection configurations 1 and 2 almost follow the same decreasing pattern with increasing engine frequency, but here configuration 2 has the lowest deflection till 18 Hz of the engine frequency. From 22 Hz to 30 Hz all configurations nearly have the same deflection and only differ by a few thousandth of a degree.

6.1.3 Torque

The steady state amplitude of the input shaft`s torque has the same pattern as figure 4.5. Again configuration 3 has the lowest torque and configuration 2 has the highest; and also the torque decrease by increasing the engine frequency.

As mentioned because deflection of the second inertia (gear box) has the first priority in designing the torsional system under consideration; the goal is to reduce oscillations in the gear box and subsequently avoid gear rattle. Therefore configurations 1 and 2 are the best choices but considering the torque amplitude configuration 2 is the desired one overall.

6.2 Dual-Mass Flywheel

6.2.1 Inertia 1

The steady state amplitude of deflection at inertia 1 in DMF system has quite the same pattern as inertia 1 in CF system. Here the second configuration has the highest deflection till 14 Hz. In this system, configuration 1 has the lowest deflection till 10 Hz but from 14 Hz configuration 3 becomes the lowest.

6.2.2 Inertia 2

At the first 4 engine frequencies (7 to 10 Hz) configuration 3 is the one that have the lowest deflection. At this time a sudden decrease in the slope can be seen from 10 Hz to 14 Hz which is due to the existence of the damping.

6.2.3 Inertia 3

Similar to the second inertia configuration 3 has the lowest deflection but this time for the first 5 engine frequencies. Again a sudden decrease is visible in the deflection diagram at 10 Hz.

6.2.4 Torque

In the DMF system steady state torque amplitude at configuration 1 has the lowest value and configuration 2 in the middle of configuration 1 and 3. Also a sudden decrease in amplitude is obvious similar to the change in deflection part of inertia 2 and 3.

Overall configuration 3 is the one chosen. However torque amplitude of the third configuration is not the lowest one but its amplitude of deflection is lower than the other configurations at inertia 2 and 3 and as was mentioned previously decreasing oscillations at the gear box is the utmost priority.

Notice that all of the sudden decreases in the slope of the indicated diagrams and also irregularities in the decreasing pattern of the deflection and torque amplitude may be due to the linear assumption of dynamic characteristics in the system; clearly it shows that to get the best effect and higher efficiency non-linear characteristics should be taken for stiffness and damping.

7 Conclusion and further research recommendations

This thesis investigates whether it is possible to lower the engine speed (down-speeding) in order to reduce fuel consumption therefore less CO_2 emissions. It is seen that DMF shows better results and facilitate the motion of inertia. The comparison of deflection at the gear box shows that there is a substantial improvement in DMFs, which are about 43% lower deflection and consequently less noise and gear rattle.

The data is acquired by assuming the mounting system as 1-DOF system, which has only one cushion instead of 5. Furthermore the torsional system has been analysed only through the engine and the gear box and the rest of the powertrain has been neglected. These assumptions give satisfying results for studying torsional system due to the fact that practically the torque amplitude after gear box (prop-shaft) is zero. Thus it will not affect the vibration of the system significantly. In order to get more accurate results it may suggest using non-linear mounting characteristics and consider the complete model of both the powertrain and the engine mounts.

As a final point it is concluded that the presented method gives satisfying results for studying the vibration of the powertrain system.

8 References

1. Thomson W.-T. (1988): *Theory of vibration with applications.* Prentice Hall, Englewood Cliffs, New Jersey.
2. Craig R.-R., Kurdila A.-J. (2006): *Fundamentals of Structural Dynamics*. John Wiley, Hoboken, New Jersey.
3. Norton, R.-L. (2004): *Design of Machinery*. McGraw-Hill, Dubuque, Iowa.
4. Rao S.-S. (2004)*: Mechanical Vibrations.* Pearson, Upper Saddle River, New Jersey.
5. Yarmohamadi H. (2009): *Towards active engine mounting systems for commercial vehicles: modeling and analysis.* LIC. Thesis. Department of Dynamics, Chalmers University of Technology, Göteborg, Sweden.
6. Walter A., Kiencke U., Jones S., Winkler T. (2008): *Anti-jerk & idle speed control with integrated Sub-Harmonic Vibration Compensation for Vehicles with Dual Mass flywheels.* SAE Technical Paper 2008-01-1737.
7. Cavina N., Serra G. (2004): *Analysis of a Dual Mass Flywheel System for Engine Control Applications.* SAE Technical Paper 2004-01-3016.
8. Jianjun H., Datong Q., Yusheng Z., Yonggang L. (2009): *Study on Natural torsional Vibration characteristics of Dual Mass Flywheel-Radial Spring Type Torsional Vibration Damper.* SAE Technical Paper 2009-01-2062.
9. Yarmohamadi H., Berbyuk V. (2008): *Computational Model of Conventional Engine Mount for Commercial Vehicles: validation and application,* submitted to Vehicle System Dynamics, February (2008).
10. Yarmohamadi H., Berbyuk V. (2008): *Dynamics of a Commercial Vehicle Engine Suspended on Adaptronic Mounting System.* Proceedings of the 9th International Conference on Motion and Vibration Control (MOVIC 2008), September 15-18 (2008), Munich, Germany.
11. Yarmohamadi H., Berbyuk V., Nilsson P., Wikenhed E., Öijer F. (2008): *Elastic, viscous and friction phenomena based computational model of engine mount dynamics*. Proceedings of the 8*th* World Congress on Computational Mechanics (WCCM8) and the 5th European Congress on Computational Methods in Applied Sciences and Engineering (ECCOMAS 2008), June 30-July 5 (2008), Venice, Italy.
12. Yarmohamadi H., Berbyuk V. (2007): *Modeling of elastomeric engine mounts for commercial vehicles.* Proceedings of the 20*th* Nordic Seminar on Computational Mechanics (NSCM 20), November 23-24 (2007), Göteborg, Sweden.
13. Singh R., Xie H., Comparin R. J. (1989): *Analysis of automotive neutral gear rattle*. Journal of Sound and Vibration 131(2), 177-196